PAPER

E-H mode transitions and high-energy electron characteristics of helical antenna coupled plasma

To cite this article: Chuansheng Wang *et al* 2021 *J. Phys. D: Appl. Phys.* **54** 315201

View the article online for updates and enhancements.

E-H mode transitions and high-energy electron characteristics of helical antenna coupled plasma

Chuansheng Wang[1,2]**, Xin Lin**[1,*] **, Fei Li**[1] **and Xilong Yu**[1,2]

[1] State Key Laboratory of High Temperature Gas Dynamics, Institute of Mechanics, CAS, Beijing 100190, People's Republic of China
[2] School of Engineering Science, University of Chinese Academy of Sciences, Beijing 100049, People's Republic of China

E-mail: linxin_bit@imech.ac.cn

Abstract

Metastable and high-energy electron characteristics obtained from optical emission spectroscopy are used to analyze the dependence of the H mode on the magnetic field strength and discharge pressure. The results show that the H-mode characteristics gradually appears as the magnetic field strength is increased, the reason being that electrons undergo multiple acceleration-collision cycles at high magnetic field strength, thereby the metastable ionization will be increased. This improves energy utilization and making the H mode appearing. The variation in the density of metastable states and the Langmuir probe data shows that the electron energy distribution function evolves from non-Maxwellian to Maxwellian. The radial constraint of the magnetic field to the electrons and thus reduces the electron heating efficiency. Moreover, the increase in electric field strength with magnetic field leads to an increase in energy obtained by the electrons per unit distance. The competition between the two makes the number of high-energy electrons decrease rapidly first, and then increase slowly with magnetic field strength increasing. The turning point increases with the increase of discharge pressure and radio-frequency (RF) power. And the higher the pressure the lower the high-energy electron. For fields between 105.5 G and 212.7 G. In the H-mode regime, and with increasing RF power, the number of high-energy electrons will be sudden rise after experiencing a steady increase. The sudden rise RF power increase with magnetic field and decrease with discharge pressure increase. However, at high magnetic fields (>265 G) and high power (>450 W), the high-energy electron density decreases with power increasing.

Keywords: helical antenna, magnetic, E-H mode transition, high-energy electrons, metastable

(Some figures may appear in color only in the online journal)

1. Introduction

Helicon plasma systems (HPSs) have wide application prospects in surface treatments [1, 2] and are exploited in space electric thrusters [3–7]. As the RF power increases, three stages arise in most HPSs: E-mode (capacitive), H-mode (inductive), and W-mode (helicon-wave) [8, 9]. The E mode is maintained by the electrostatic field that induced by the end voltage drop caused by the antenna resistance. The H mode is a discharge maintained by the coupling between the electric field that induced by the antenna current and the plasma. The W mode plasma generated by the coupling of the helicon wave and plasma. W mode discharge mechanism is essentially different from the other two discharges. When a mode transition occurs, the plasma parameters change abruptly in

value. These changes affect the circumstances of the application significantly. Therefore, in facilitating the generation and control of the plasma, understanding the mechanism underlying each transition is necessary, as is its dependence on those parameters.

There are three main differences between HPS and inductively coupled plasma (ICP): (a) the axial component of the applied magnetic field, (b) the antenna structure causing changes in the excitation field [10], and (c) the low discharge pressure in the HPS. Therefore the mechanism driving the E-H mode transition and the mechanism behind the H mode ionization in HPSs have differences from that for ICP discharge [11]. There is a lack of sufficient studies concerning changes in the H-mode mechanism with magnetic field strength and discharge pressure in HPSs.

Studies of the E-H mode transition for ICP discharge [12, 13] in the absence of a magnetic field show that discharge pressure [14–16], source frequency (radio frequency band) [17], and gas composition [18–22] influence mode transition density and mode transition power threshold [14, 18, 23, 24] during mode transition. Several different mechanisms have been proposed to explain these influences. In the explanation of the discharge mechanism, it is believed that multi-step ionization as represented by metastable ionization is increased. Thereby, reducing the collisions loss and improving the energy utilization is an important ways to maintain the H-mode discharge [25–28]. Through calculations, Zheng *et al* [29] also found that the addition of metastable states significantly affects the plasma electron temperature and electron density trends with low magnetic field strengths (<60 G). They showed that regardless of whether there is a magnetic field, the metastable state is an important feature affecting ionization. The presence of a static axial component of the magnetic field also affects plasma properties [30, 31], which results in a plasma anisotropy that complicates discharges. Generally, the metastable state is believed to be produced through the collisions of high-energy electrons with ground-state particles [32, 33]. Therefore, the process of generating high-energy electrons has a significant effect on discharges. Chung *et al* [34] found by observing the electron energy distribution function (EEDF) for the H-mode, the low-energy electrons in a weak magnetic field (<20 G) undergo electron-cyclotron-resonance (ECR) heating, that increases their heating efficiency significantly. Godyak *et al* [35] further found that the effect of ECR on low-density plasma produces a greater contribution to plasma heating, but when the density increases, ECR-induced heating weakens. Lee *et al* [36] established a coupling model for the discharge power of a planar coil under a weak magnetic field, and believe that the excitation of the plasma wave is one of the reasons causing additional electronic damping. Furthermore, when the axial magnetic field is high (above 100 G), the helicon wave mode appears under high power, and the role of high-energy electrons is more prominent [11, 37–39]. Therefore, the strength of the external magnetic field significantly affects the electron heating mechanism, which in turn affects the ionization process.

In this article, the dependence on magnetic field strength and discharge pressure of the H mode in the helicon antenna
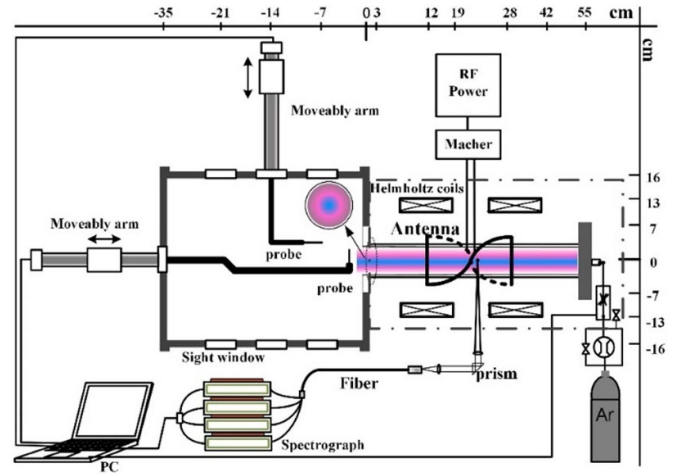

Figure 1. Schematic of the helicon plasma experiments.

coupling plasma. The metastable state density and high-energy electron data obtained from the optical emission spectroscopy [32, 40–43] is used to qualitatively analyze the cause of the H mode under high magnetic fields. Section 3 presents the E-H transition characteristics and explanations. Section 4 focuses on the analysis of the changes in the high-energy electron detector (HEED) with magnetic field and discharge pressure. Section 5 studies the dependence of the metastable state on magnetic field strength and discharge pressure for the E and H modes.

2. Experiment setup and measurement methods

2.1. Experiment setup

As shown in figure 1, the aluminum alloy vacuum chamber has an outer diameter of 340 mm and length of 350 mm. The background vacuum of the chamber is approximately 5×10^{-5} Pa. A mechanical pump (TRP-24, Beiyi Woosung Vacuum, Technology, Beijing) and a molecular pump (CFB-600, Chuanbei Vacuum Technology, Beijing) with pumping speeds of $6 \, l \, s^{-1}$ and $600 \, l \, s^{-1}$, respectively, were used to maintain the vacuum. The ionization tube is a quartz tube with an outer diameter of 70 mm and a length of 520 mm. This tube connects to the vacuum chamber at one end and sealed at the entrance using an aluminum flange. A helical antenna of length 180 mm and outer diameter 80 mm is coiled externally around the quartz tube. A 2 kW, 13.56 MHz RF power supply (RSG2000, Rishige, China) connects to this antenna through a π-type matching box. Argon is the ionization gas and is controlled by a mass flow controller (F-201CV-050-AGD-33-V, Bronkhorst, The Netherlands). A simple adjustment of the flow rate allows the discharge pressure in the chamber to be varied from 0.01 Pa to 10 Pa.

The axial component of the static magnetic field is generated using two electromagnetic coils connected in series, enabling a sustained operation of more than 1.5 h. Magnetic field strengths between 0 G and 400 G were possible by adjusting the current in the coils from 0 A to 8 A; given
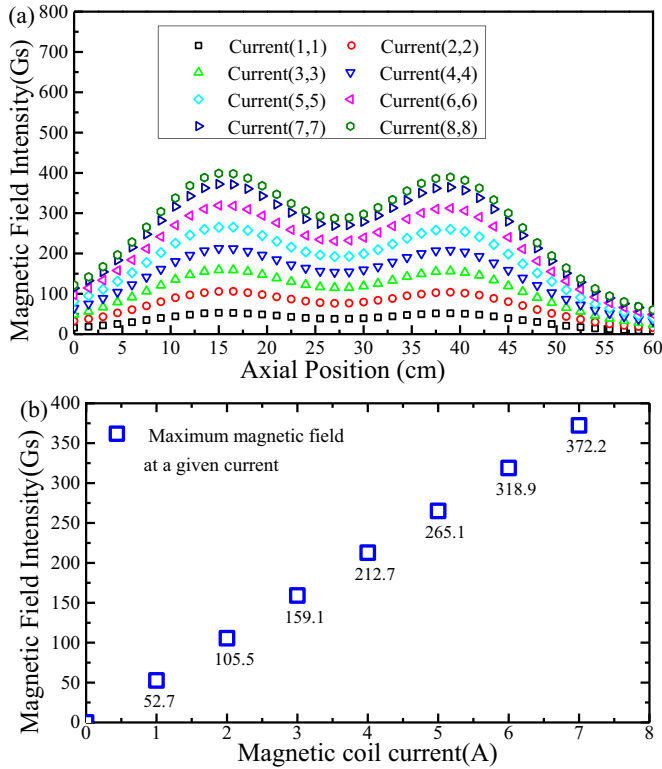
Figure 2. Attributes of the axial component of the magnetic field: (a) field profiles along the central axis for the seven coil current settings, and (b) current dependence of the field at the peak location, 15 cm along the central axis.

Figure 3. Emission spectrum of Ar plasma.

the axial magnetic field distribution (figure 2(a)), the magnetic field strength generated by the coil is represented by the maximum values at a location 15 cm along the central axis (figure 2(b)). For example, with a coil current of 2 A, the magnetic field strength is 105.7 G.

Three discharge pressures (0.23 Pa, 0.33 Pa, 0.43 Pa) and seven coil currents (0–6 A, in steps of 1 A) constitute the different settings in our study, the corresponding magnetic field strength ranges from 0 G to 318 G, in steps of 52.6 G.

2.2. Optical emission spectroscopy

In low-pressure RF plasma, electron impact excitations from the ground state to the excited states (Ar*) are the dominant excitation channels in plasma production. During de-excitations, the excited atoms release photons for which the emission intensity I_{ij} associated with the decay of the excited state j to state i is [42]: $I_{ij} = K_{ij}A_{ij}n_{Ar_j}hc/\lambda$, where K_{ij} denotes the spectrometer factor including the CCD response, A_{ij} the Einstein coefficient, n_{Ar_j} the Ar_j level density, c the speed of light in vacuum, h the Planck constant, and λ the wavelength. In this study, a telescopic system and an aperture grating were used to collect plasma photoemissions received at a location 22 cm from the central axis of the quartz tube and inputted into a four-branched multichannel spectrometer (AvaSpecULS3648, Avantes, The Netherlands) with a resolution of 0.1 nm at full-width at half-maximum; its spectral acquisition
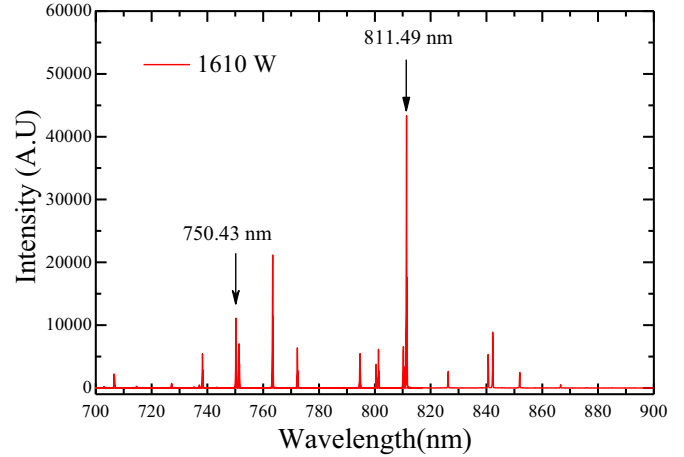
range is between 360 nm and 900 nm. The plasma lines for argon atoms mainly come from the 4p–4s state transition, which are concentrated between 700 and 900 nm (figure 3).

Several characteristic spectral lines of Ar were selected to trace the mode transitions and other plasma parameters. For neutral Ar atoms, the following reactions have to be considered:
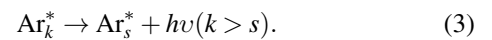
(a) direct excitation by electron collision,

$$e + \text{Ar} \rightarrow e + \text{Ar}_i^*; \qquad (1)$$
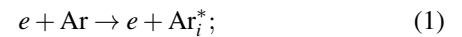
(b) indirect excitation by electron collision,

$$e + \text{Ar}_m^* \rightarrow e + \text{Ar}_j^*; \qquad (2)$$
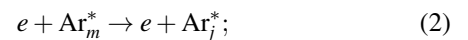
(c) radiative cascade,

$$\text{Ar}_k^* \rightarrow \text{Ar}_s^* + h\upsilon(k > s). \qquad (3)$$

In general, the upper energy levels of a spectrum are generated by direct and indirect excitations, whereas for excited states the probability is different because cross sections differ. Table 1 shows the excitation data for the two main spectral lines from Ar ionization. For the 750.43 nm line ($2p^1 \rightarrow 1s^2$), the indirect collision cross section is small, and thus the direct collision excitation is the main process in plasma generation, whereas the most effective excitation channel for the 811.49 nm line ($2p^9 \rightarrow 1s^5$) is from the $1s^5$ metastable collision excitation. These two lines are normally used to characterize mode transitions [8, 42, 44]. Note that, if the metastable state density is greater than 10^{10} cm^{-3}, and the real line strength needs to be used; the self-absorption of the 811.49 nm line must be considered [45–47]. However, this circumstance does not affect the trend in the variation in spectral line intensity with the metastable state density. The 750.43 nm spectral line is not reabsorbed, hence the actual spectral ratio for the

Table 1. Excitation data for the two main spectral lines from Ar ionization, E_{th} excitation threshold, σ_{max} maximum collision cross section.

λ (nm)	Direct excitation		Indirect excitation		A_{ij} (10^6 s^{-1})	K_{ij}
	E_{th} (eV)	σ_{max} (10^{-19} cm^2)	E_{th} (eV)	σ_{max} (10^{-16} cm^2)		
750.43	13.48	111	1.6	0.14	44.5	0.108
811.49	13.08	(130)	1.53	25	33.1	0.053

811.49/750.43 nm lines is higher than the present value, but the overall trend remains unchanged.

Given the above definition of the spectrum emission intensity, we suppose particles of the upper energy level only transition to the lower energy level by radiation emission. Then, the higher the density of the upper energy state, the stronger the line intensity. In low-temperature plasma, the upper state is mainly produced by electron collisions; see equation (1). If the low-energy state is the ground state, it is assumed to be stable. When the discharge reaches equilibrium, the generation rate of Ar_i^* is equal to the attenuation rate, and hence the emission intensity of the spectral line is expressed as $I_{spec} = n_e K_{ij} A_{ij} \tau_{Ar} k_{Ar} [\mathrm{Ar}] \frac{hc}{\lambda}$, where I_{spec} denotes the intensity of a specific spectrum, τ_{Ar} the life length of excited state, n_e electron density, k_{Ar} the chemical reaction rate, and the other parameters have the same meaning as above. That is, the variation in the spectral intensity indicates changes in the electron density, with energy being higher than the excitation threshold of the spectral line. The excitation threshold of the 750.43 nm spectral line is 13.48 eV and is used to analyze the changes in the HEED. Metastable ionization is an important process in multiple-step ionization. According to Czerwiec [42], the variation in the 811.49/750.43 nm spectral line ratio can be used to characterize the change in number density of the metastable states, its expression being

$$\frac{I_{811.49}}{I_{750.43}} = C\left(\frac{k_{811.49}^{dir} n_{Ar} + k_{811.49}^{m} n_{Ar}^{m}}{k_{750.43}^{dir} n_{Ar} + k_{750.43}^{m} n_{Ar}^{m}}\right), \qquad (4)$$

where k^{dir} and k^m denote rate coefficients of the reaction associated with excitations from the ground state to the metastable states of densities n_{Ar} and n_{Ar}^m, respectively, and C denotes the spectrometric response coefficient. With a low degree of ionization, the ground state is considered stable, and the 750.43 nm spectral line intensity produced by transitions to the metastable state is small. At the same time, the ratio of the reaction rate coefficients is monotonic and small [26]. Therefore, equation (4) can be approximately written as

$$\frac{I_{811.49}}{I_{750.43}} \propto \frac{k_{811.49}^{dir} n_{Ar} + k_{811.49}^{m} n_{Ar}^{m}}{k_{750.43}^{dir} n_{Ar} + k_{750.43}^{m} n_{Ar}^{m}} \rightarrow \frac{k_{811.49}^{dir}}{k_{750.43}^{dir}} + \frac{k_{811.49}^{m}}{k_{750.43}^{dir} n_{Ar}} n_{Ar}^{m}. \qquad (5)$$

Clearly, this spectral line ratio is linearly related to the metastable state density. Its form is the same as equation (4) in [42].

3. Variation of the E-H mode transition characteristics with magnetic field strength

Figure 4 presents the mode transition lines intensity variation with power for different magnetic field strengths obtain by
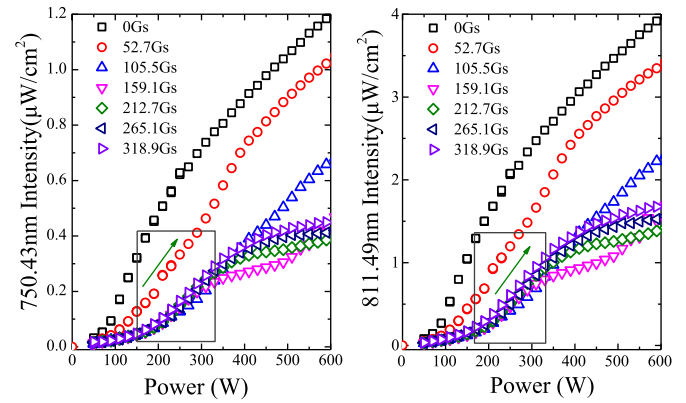
Figure 4. Dependence of the 750.43 nm (left) and 811.49 nm (right) spectral line intensity on RF power for different magnetic field strengths; discharge pressure is set at 0.23 Pa.

experimental methods. Generally, when inductively coupled discharge takes place with no magnetic field, at high pressure (such as, above 10 Pa) as E→H occurring, the characteristic spectral line intensities (750.43 nm and 811.49 nm) is jump; when the pressure is low (such as, below 1 Pa), there is no typical H modal behavior [8, 26]. With no magnetic field present (see figure 4), the intensity of the spectral lines increases quickly and smoothly with increasing RF power; no mode transition occurs. With the magnetic field strength set at 52.7 G (coil current is 1 A), the slope of the spectral intensity is different in the three ranges of power 0–200 W, 200–350 W, and 350–600 W. Nevertheless, the mode transition is not distinguishable. With a magnetic field strength of 105.5 G (2 A), the variation in intensity for the 750.43 nm and 811.49 nm lines with increasing RF power indicates that the E-mode is present when the RF power is below 200 W; the discharge enters the mixed mode regime (E + H, inside the grey box in figure 4), but the typical H-mode does not appear. With magnetic field strengths above 105.5 G (coil current above 2 A), the discharge goes through three ionization stages (E, E + H, and H-modes) in sequence with increasing RF power. With densities above 159.1 G (3 A), the H-mode characteristics are obvious. Indeed, after the RF power exceeds 350 W, the discharge enters the H-mode regime.

The increases in the multiple-step ionization channel from the Ar metastable states is one of the main reasons that plasma operations exploit the H-mode [27, 28]. The high efficiency utilization rate of energy in multi-step ionization is determined by this basic physical process and does not depend on how the plasma is generated. As is well known, the metastable ionization threshold of argon is approximately 4.2 eV (representing the energy difference between metastable state (11.5 eV) and
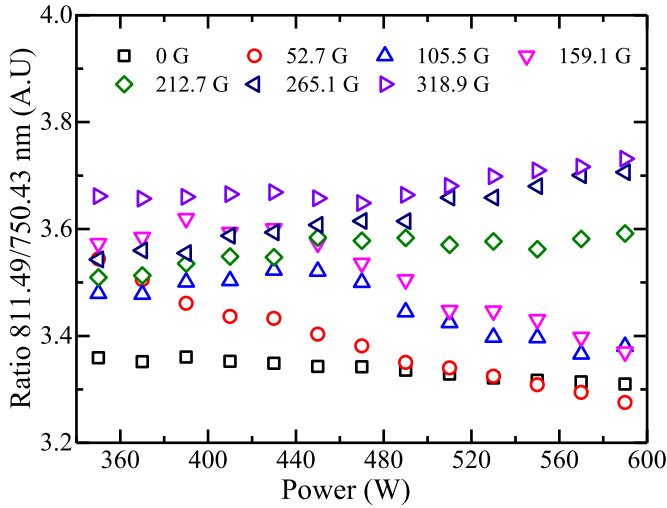
J. Phys. D: Appl. Phys. **54** (2021) 315201

C Wang *et al*

Figure 5. Variation in metastable against RF power for different magnetic field strengths. Taking 212.7 G as the dividing point, above 470 W, when the magnetic field strength is greater than 212.7 G, the metastable state density increases with power, and vice versa.

Figure 6. Under the restraint of the axial magnetic field, an electron undergoes multiple acceleration-collision processes, which enhance the multi-step ionization process represented as metastable ionization.

ionized state (15.7 eV)). Therefore, the number of electrons with energies over 4.2 eV and the number of metastable states are determined the contribution from multiple-step ionization to the total ionization.

The variation of the metastable density with magnetic field strength is obtained from the ratio of the 811.49/750.43 nm line intensities (as shown in figure 5). This variation shows that, when the magnetic field is not present, the density of the metastable state is low and the contribution from multiple-step ionization to the total ionization is not significant. Hence, the H-mode does not appear. The effect of a strong magnetic field on electrons is similar to that for elastic collision, which increases the probability of electrons being continuously accelerated. Therefore, subject to a Lorentz force, the electrons undergo a spiral motion along magnetic field line. As they spiral, the electrons are accelerated by the axial and angular components of the electric field. After some time in this field, the electrons acquire enough energy that, when they collide with argon atoms in the ground state, they produce a metastable state. Moreover, because electrons can undergo multiple stages of spiral acceleration, the probability of multiple metastable states production increases. The density and generation rate of the metastable states therefore increase with magnetic field strength.

Because of the inhomogeneity of the magnetic field in this experiment, some low-energy electrons undergo resonant heating [34, 35] in low magnetic field (<50 G). More importantly, in the discharge area of high magnetic field, lower energy electrons gain energy that exceed 4.2 eV from spiral acceleration and collide with metastable particles, which results in indirect ionization (as shown in figure 6). During the first period of collisions, the electrons do not reach the wall and undergo repeated acceleration-collision cycles under the remaining energy until reach the wall and become lost. This process enhances multiple-step ionization significantly. Therefore, the magnetic field intensifies multiple-step
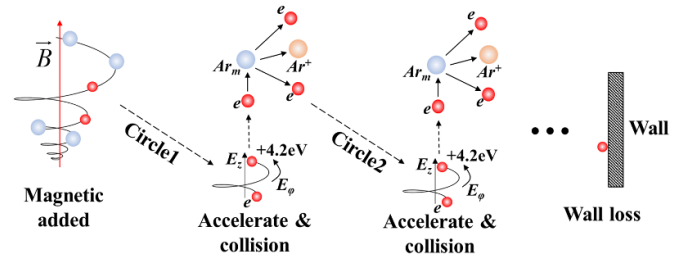
ionization by increasing the number of acceleration-collision-ionization cycles. With the combined increase in electron collisions and metastable states, multiple-step ionization is enhanced; that is, the stronger the magnetic field is, the more prominent are the H-mode characteristics.

4. Properties of the HEED

4.1. Variation with magnetic field strength

From the above analysis, the combined effect of the external magnetic field and the electromagnetic field induced during mode transition, the high-energy electrons lose their non-local characteristics with the axial magnetic field added. This decreases the radial flux and changes the mechanism driving the plasma energy balance. Therefore, studying the relationship between magnetic field strength and high-energy electrons is necessary.

From the variation in field strength with coil current, we extracted the data for the two low RF power values (130 W and 190 W) to reflecting the variation of the HEED with magnetic field strength in the E-mode, and the intermediate power data (330 W) to reflect the mixed mode variation. The two high RF power values (450 W and 550 W) are used to extract the H-mode variation with magnetic field strength.

Figure 7 shows the variation of the 750.43 nm spectral line intensity with magnetic field strength under different discharge modes in three discharge pressures. Here, the line intensity decreases, which implies that the high-energy electron production efficiency decreases. That means the magnetic field inhibits the generation of high-energy electrons. At fixed pressure 0.23 Pa, increasing the magnetic field strength from 0 G (0 A) to 105.5 G (2 A) reduces rapidly the intensity of the 750.43 nm lines for the E-mode. With magnetic field strength above 105.5 G (2 A), the line intensity remains unchanged or increases slowly. This indicates a turning point at which, in 0.23 Pa discharges and magnetic field strengths above 105.5 G the number of high-energy electrons diminishes. The mixed mode exhibits the same trend as the E-mode. In the H-mode, with the magnetic field strength below 159.1 G (3 A), the intensity of the 750.43 nm line decreases rapidly with increasing magnetic field strength, whereas above 159.1 G (3 A), the intensity gradually increases. At 159.1 G (3 A), the intensity of the spectral line is at a minimum value.
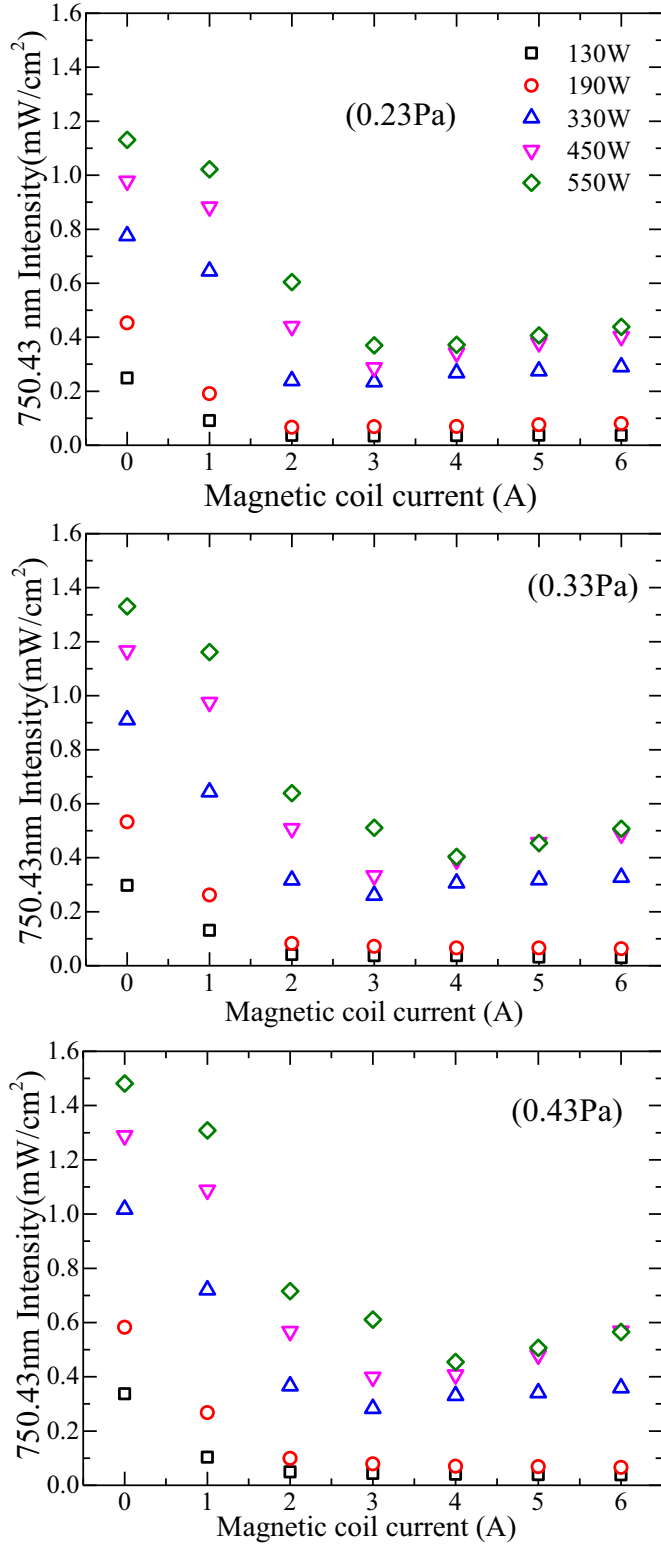
Figure 7. Variation of the 750.43 nm line intensity with coil current for various RF power: (a) 0.23 Pa, (b) 0.33 Pa, (c) 0.43 Pa. The high-energy electrons decrease first and then slowly rise with increasing magnetic field strength.

To understand the reason for the decrease in the HEED when the magnetic field is applied. The radial distribution of the electric field strength is calculated by HELIC code [48, 49] to analysis the energy transfer between electrons and electric

Table 2. Calculation parameters.

Items	Parameters
Plasma radius (R_p)	0.032 m
Wall radius (R_w)	0.15 m
Antenna type	Half helix
Antenna length (L_A)	0.18 m
Power frequency	13.56 MHz
Wave number	1
Ion species	Ar^+
Axis density	5×10^{17} m^{-3}
Electron temperature	3 eV
Pressure	3 mTorr
Static magnetic field	1 G, 150–300 G
Collision factor	1
Zp	0.002 m

field. Over the RF power range for the H mode, the radial uniformity of the plasma is extensive. The profile of the radial distribution for the plasma was adjusted using a three-parameter equation, specifically,

$$\frac{n(r)}{n_0} = \left[1 - \left(\frac{r}{\omega}\right)^s\right]^t, \omega = \frac{R_p}{\left[1 - (f_a)^{1/t}\right]^{1/s}}, \quad (6)$$

where $n(r)$ denotes the plasma density, n_0 neutral gas density, r the radial position, R_p the plasma edge position, f_a a parameter to control plasma width, and s and t parameters to adjust the plasma edge gradient and the internal gradient of the plasma, respectively. From the discharge settings used in this study, the three parameters governing the radial distribution of the plasma density are set to $f_a = 0.01$, $s = 6$, and $t = 0.5$. Other specific settings of the conditions are listed in table 2.

Curves of the radial distribution of the electric field for various magnetic field strengths obtained under the given calculation conditions are present in figure 8. Generally, the electric field of 2.8–3.2 cm in figure 8 is generated by TG wave and the electric field in body plasma (0–2.8 cm) is generated by helicon wave. The curve for field strength 1 G is used as reference. At 1 G, the radial and angular components of the electric field are close to 0, whereas the axial component has values greater than those under other magnetic field conditions within a 2.8 cm range, which indicates that there is no excitation of plasma waves. Near the axial location (figure 8), the radial and angular components of the electric field strength E_r and E_φ are ten times greater than the axial component E_z. However, the axial magnetic field confines the radial movement of electrons implying the radial component of the electric field contributes little in accelerating the electrons. That is, the most efficacious direction for electron heating is limited. Consequently, the number of energetic electrons is reduced considerably.

The experimental results for pressures 0.33 Pa and 0.43 Pa (figures 7(b) and (c)) show that the variation of HEED by the 750.43 nm line intensities with increasing magnetic field is similar to that for 0.23 Pa. The turning point for the E-mode is 105.5 G (2 A). Unlike at 0.23 Pa, the turning point for the mixed mode is 159.1 G (3 A). In the initial stage of the H-mode, the turning point is 159.1 G (3 A). However, with
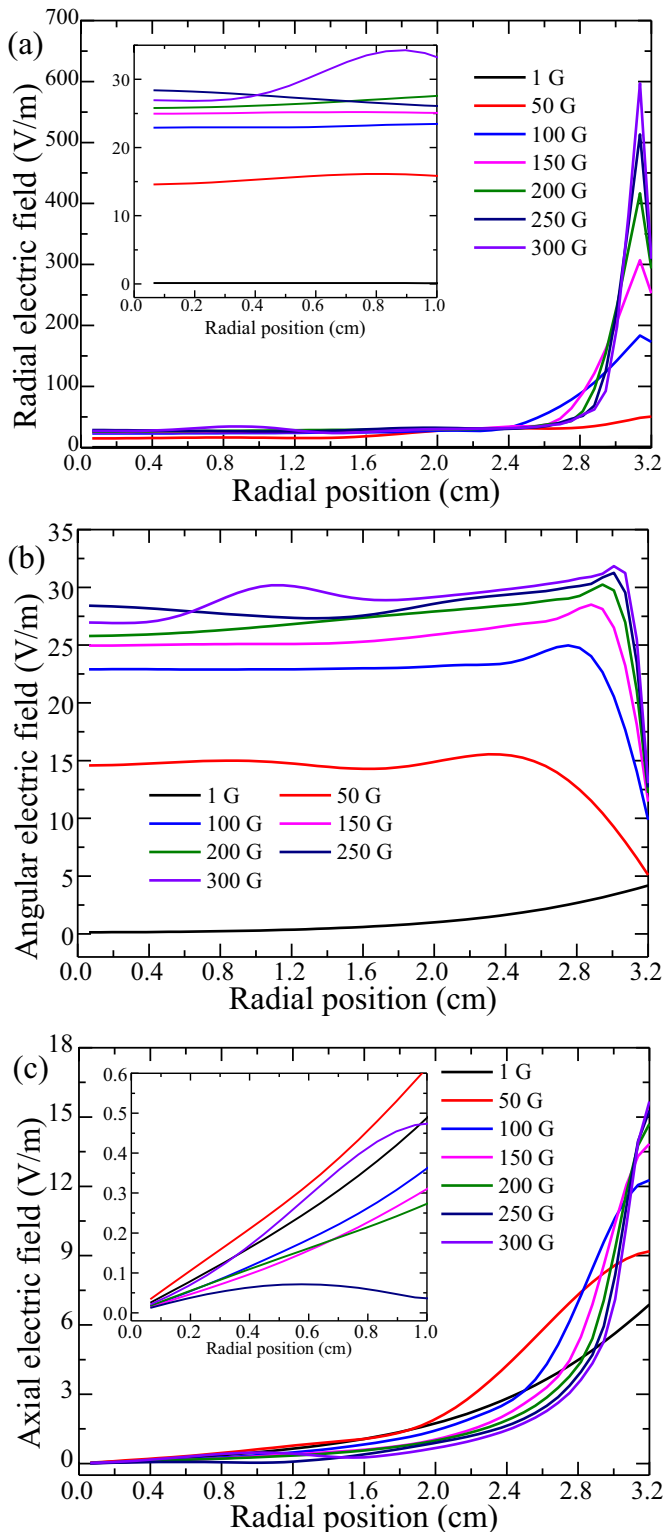
Figure 8. Electric field strength as a function of (a), (b) radius over different intensity scales and RF power for various magnetic field strengths. The data at 1 G are used as a comparison for other magnetic field settings.

an RF power of 550 W, the turning point is 212.7 G (4 A). The analysis shows that the main reason is that with increasing power, there is an increase in the electric field excited by the antenna, and an increase in the energy obtained by the
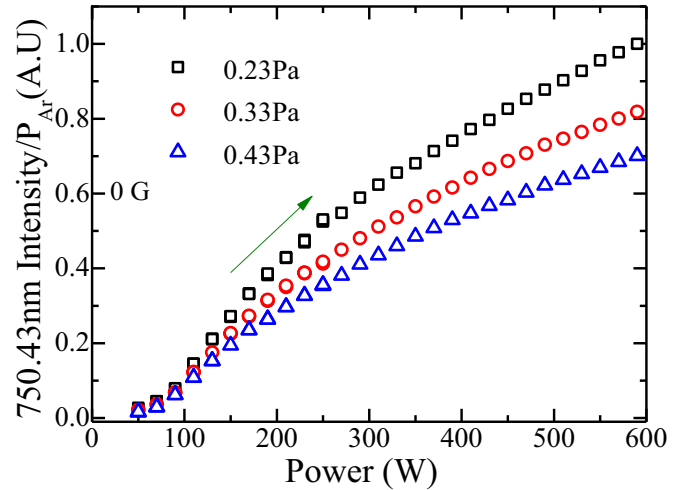

Figure 9. Variation in the normalized line intensities against RF power for different pressures and no magnetic field.

electrons per unit distance. Hence, at high power, the turning point in suppression shifts to 212.7 G (4 A).

From the calculations, the electric field strength gradually increases, as the magnetic field increases, and hence the energy gained by electrons per unit path length increases. Therefore, the relationship that magnetic field constraint of the radial movement of electrons and the enhancement of electric field strength cause high-energy electrons to rapidly decrease first and then slowly increase as the magnetic field increases.

4.2. Variation with pressure

As is well known, direct ionization and metastable state generation are associated with high-energy electron collision. Pressure has an important influence to high-energy electron production by changing mean free path. We next explore the influence of pressure on these high-energy electrons produced by a helical antenna. The curves in the figures are all normalized by the maximum value in each subgraph to analyze the influence of discharge pressure on the HEED intensities and RF power.

Figure 9 shows the intensity curve for the HEED intensity against RF power for different discharge pressures expressed using the intensity of the 750.43 nm Pa^{-1} spectral line at zero magnetic field. With increasing discharge pressure and constant power, the 750.43 nm PAr^{-1} line intensity decreases. Moreover, the line intensity curves for the three pressures have similar trends, implying the change in pressure in the 0.23–0.43 Pa range has no influence on the plasma coupling characteristics. When the RF power is below 200 W, the efficacy in high-energy electron generation is greater than that for RF powers above 200 W. Comparing the decrease in high-energy electrons between 0.23–0.33 Pa and 0.33–0.43 Pa, we see that their rate of decrease in the HEED decreases with increasing pressure.

At the same time, the effect of discharge pressure on HEED intensities when a magnetic field is applied was studied. Figure 10 shows the normalized 750.43 nm Pa^{-1} line intensity

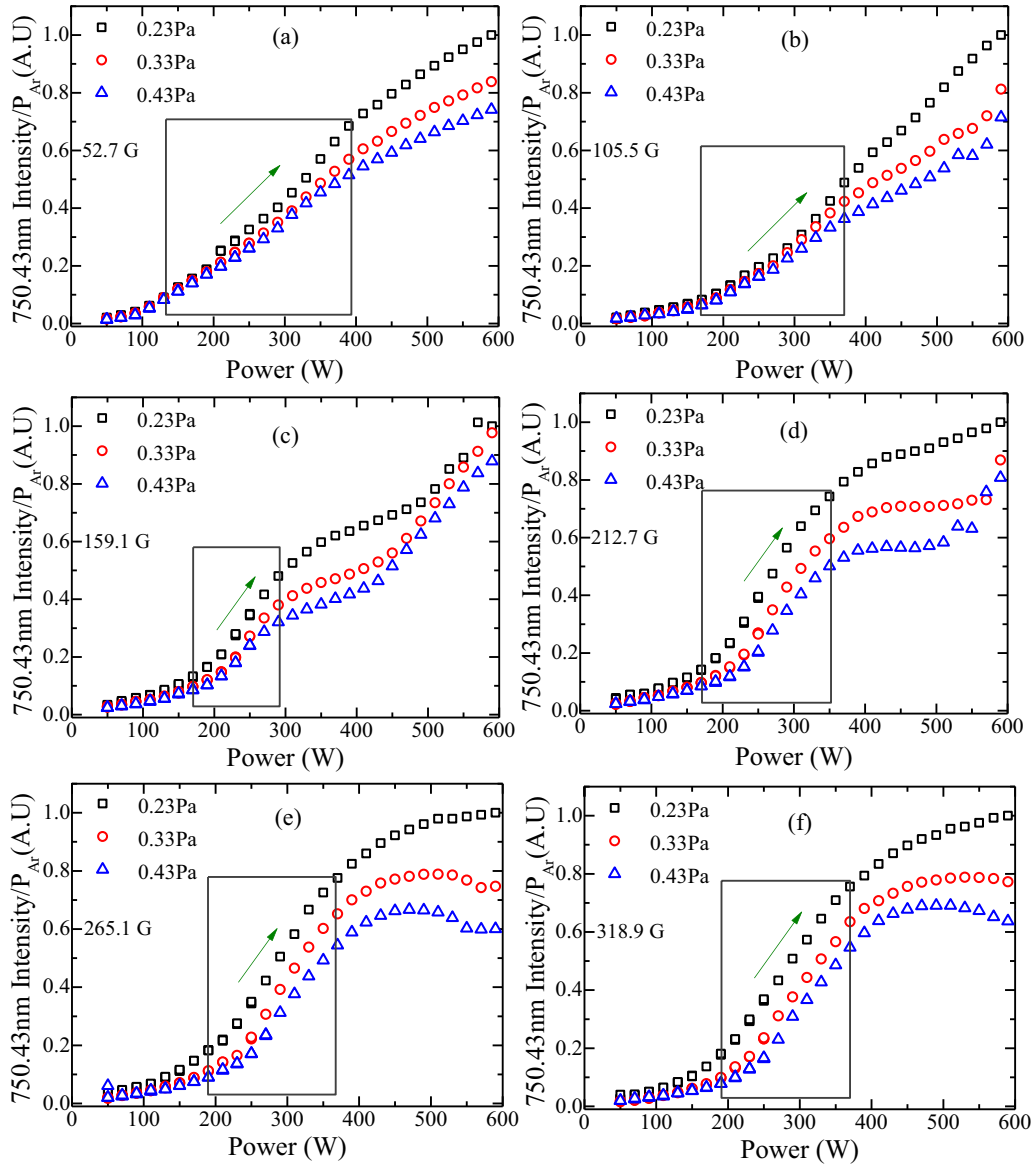J. Phys. D: Appl. Phys. **54** (2021) 315201

C Wang *et al*

Figure 10. Variation of the normalized 750.43 nm line intensity against RF power for three pressure settings and different magnetic field strengths: (a) 52.7 G, (b) 105.5 G, (c) 159.1 G, (d) 212.7 G, (e) 265.1 G, and (f) 318.9 G. The framed box marks the mixed mode regime.

against RF power for the same three pressure settings and different magnetic field strengths from 52.7 G (1 A) to 318.9 G (6 A).

The result is similar to that for mode transitions (as discussed in section 3) that occur when the magnetic field strength is above 105.5 G (2 A). Comparing figures 10(a) and (b), the H-mode gradually appears and expands, with increasing magnetic field strength. For example, the data for 0.33 Pa shows that when the magnetic field is 105.5 G, the H mode is almost non-existent. When the magnetic field is 159.1 G, the H mode continues from 330 W to 400 W, the RF power range is 70 W, and when the magnetic field is 212.7 G, The H mode continues from 370 W to 570 W, and the power range is 200 W. When the magnetic field strength is above 212.7 G (4 A), the H-mode expands under a RF power of 600 W. The transition power

threshold from the E-mode to the mixed mode is approximately 200 W. With magnetic field strength increasing from 159.1 G to 318.9 G, the transition threshold from the mixed mode to the H-mode changes from 300 W to 400 W. At or below 105.5 G (2 A), the slope of the curve differs in the different ranges in RF power, but no significant changes in mode transition characteristics appear. That is, the coupling effect of magnetic field and high-density plasma is stronger, and the effect of the magnetic field during the discharge process of a high-electron-density plasma is more significant.

As shown in figures 10(a) and (b), when the magnetic field strength is lower than 105.5 G, the curves for the normalized spectral line intensity show that the HEED decreases with increasing discharge pressure when the RF power is below 350 W. Moreover, the three curves are very close, which
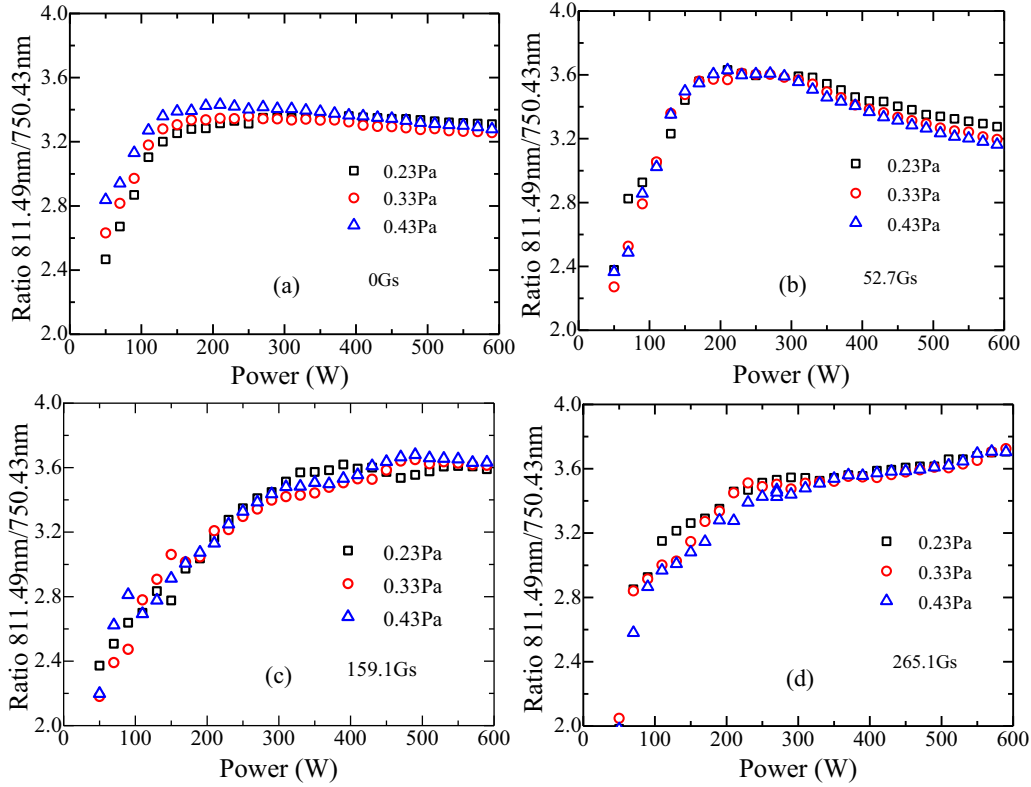
J. Phys. D: Appl. Phys. **54** (2021) 315201

C Wang *et al*

Figure 11. Variation of line ratio against RF power for the three prescribed discharge pressures at different magnetic field strength, (a) 0 G, (b) 52.7 G, (c) 159.1 G, and (d) 265.1 G.
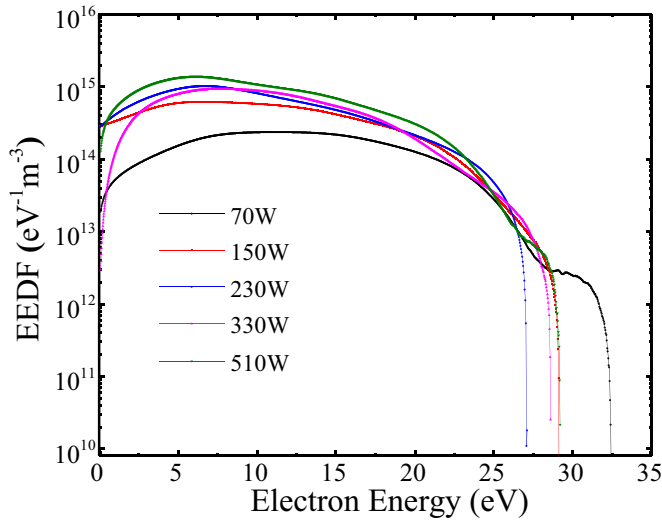

Figure 12. Log-normal plot of the electron energy distribution versus electron energy for different RF powers at fixed pressure 0.33 Pa and no axial magnetic field.

implies that the pressure has little influence on HEED. When the power is above 350 W, the HEED decreases significantly as the pressure increases. With magnetic field strengths between 159.1 G (3 A) and 212.7 G and with increasing RF power, high-energy electrons initially increase slowly in number in the E mode regime, then increase rapidly in the mixed mode

regime, slow after entering the H mode, and finally increase rapidly. With increasing magnetic field strength, the RF power associated with high-energy electron generation increases rapidly, and when the pressure increases, this power decreases. For example, the power corresponding to the rapid increase in HEED at 0.43 Pa is 430 W at 159.1 G, and 510 W at 212.7 G. At 159.1 G, the power when the HEED suddenly increases was reduced from 490 W at 0.23 Pa to 430 W at 0.43 Pa.

Recalling section 2.2, the excitation threshold of the 750.43 nm line is 13.48 eV [42]. Therefore, the excited electrons that generate the 750.43 nm spectral line are electrons with energies greater than 13.48 eV. At 159.1 G, when the discharge power exceeds a certain value, the energy obtained by electrons close to the excitation threshold under the combined action of the static magnetic field and the electric field over their effective mean free path exceeds the excitation threshold of 13.48 eV. At this moment, the cyclotron radius is larger, and hence the collision frequency for electrons and neutral particles under the action of the magnetic field is higher. Therefore, the spectral line intensity rises rapidly above a certain power threshold, which is the power at which the intensity rapidly increases for the H-mode. With increasing discharge pressure, the effective mean free path for electrons decreases. In the high magnetic field (265.1 G and 318.9 G), when the discharge power is greater than 450 W, the number density of high-energy electrons decreases with increasing power. One possible reason is the weakening of the heating effect at the ECR at high magnetic field strengths and high densities [34].
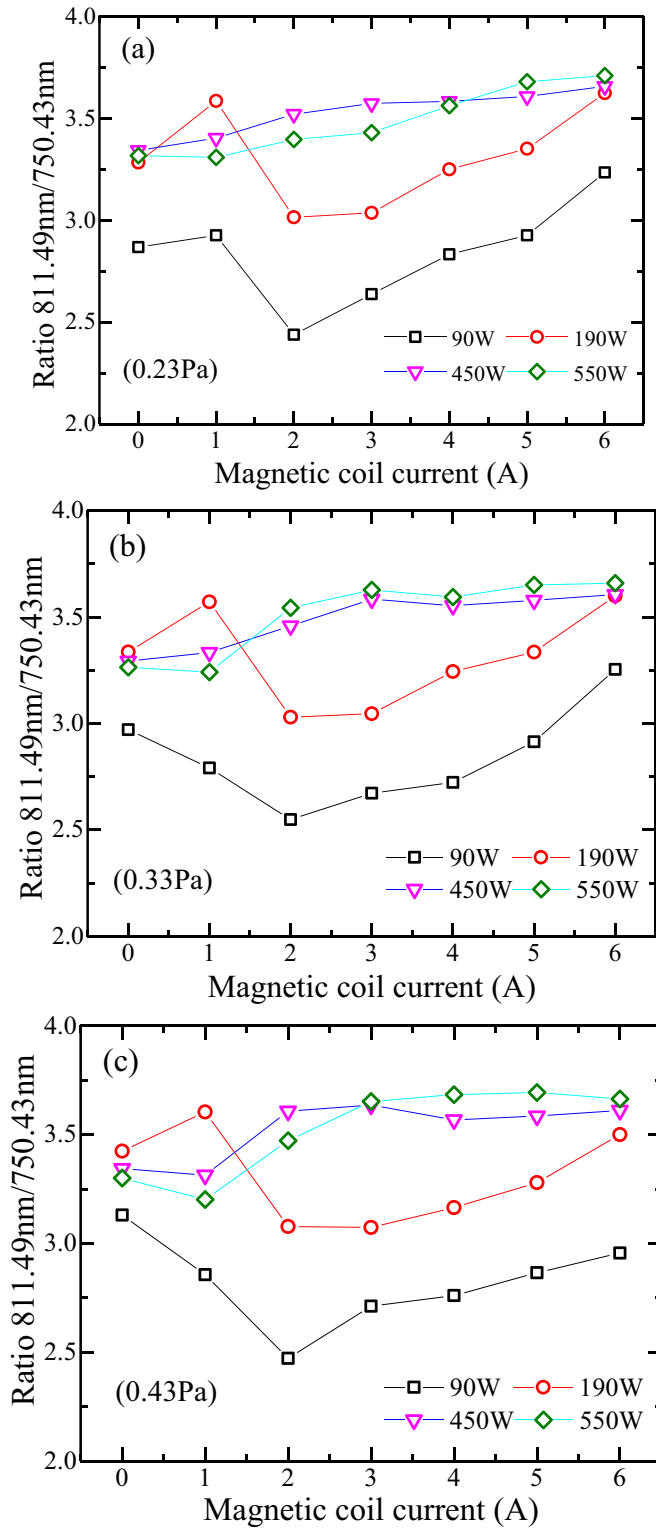
Figure 13. Variation in line intensity ratio as a function of coil current for various RF powers, (a) 0.23 Pa, (b) 0.33 Pa and (c) 0.43 Pa.

As well as changes in the electromagnetic waves propagating in the plasma and other reasons such as the weakening of the power coupling efficiency of the nonlinear action, the HEED decreases with increasing power. This specific mechanism needs to be further analyzed.

5. Properties of the metastable states

5.1. Influence of the pressure and magnetic field on metastable states

From the analysis in sections 4.1 and 4.2, the magnetic field strength and pressure have a significant effect on the HEED that results in the generation of metastable states, and hence affects the balance in plasma ionization. This section explores the dependence of the metastable state density on pressure and magnetic field strength. The experimental results are shown in figure 11. At zero magnetic field, if the power is below 200 W, the density of metastable states increases rapidly and non-linearly with increasing power. Above 200 W, this density decreases slowly with increasing power. If the power is below 250 W, the density increases with increasing pressure. If the power is above 250 W, this density gradually decreases and tends gradually to the same value for the three pre-specified pressures, which indicates that density and pressure are weakly related.

Because the spectral line ratio is closely related to the EEDF, then when the discharge power increases to 200 W, the metastable state increases rapidly, which indicates that the fraction of low-energy electrons of the total electrons increases rapidly (as shown in figure 11(a)). When the discharge power is higher than 200 W, the density of the metastable state increases slightly; that is, the ratio of high and low energy electrons is stable. Therefore, as the power increases, the EEDF changes from a non-Maxwell distribution to a Maxwell distribution. To verify this conclusion, as shown in figure 12, we plotted the curve for the EEDF against power at a discharge pressure of 0.33 Pa as measured by the Langmuir probe [42, 50, 51]. Langmuir probe data shows that the EEDF transitions gradually from a Druyvesteyn-like distribution at low power to a Maxwell-like distribution at high power.

As shown in figures 11(b)–(d), with an applied magnetic field, the density of metastable states is unchanged with increasing pressure at low RF power (i.e. 250 W). At higher power, and for magnetic field strength 52.7 G (1 A), the density of the metastable state decreases with increasing power and decreases slightly with increasing pressure at high RF powers. Moreover, the density increases with increasing RF power and remains unchanged with increasing pressure and a magnetic field strength of 265.1 G (5 A).

5.2. Influence of magnetic field for E- and H-modes

We next investigate the influence of the magnetic field strength for three discharge pressures on the density of the metastable state for the E and H modes. The curves of the line intensity ratio against coil current at RF power 90 W and 190 W (as shown in figure 13) are used to characterize the changes in the metastable state for the E-mode with increasing magnetic fields. Similarly, the curves for 450 W and 550 W characterize the changes in the metastable state in the H-mode.

If the magnetic field strength is above 105.5 G (2 A), the density of metastable states increases with power increasing; moreover, with increasing magnetic field strength, this density

increases for the E-mode, whereas for the H-mode, it remains basically unchanged. If the magnetic field strength is below 105.5 G (2 A), at the beginning of discharge (90 W) and under low pressure (0.23 Pa), the density of metastable states first increases and then decreases, whereas for 0.33 Pa and 0.43 Pa, this density continues to decrease. When approaching the threshold power for mode transition (190 W), the density first increases and then decreases with increasing discharge pressure. The peak values of the density appear at a magnetic field strength of 52.7 G (1 A), the maximum peak value being greater than that for the H-mode. If the discharge enters the H-mode, at lower power (450 W), and for 0.23 Pa and 0.33 Pa operating settings, the density gradually increases with increasing magnetic field strength, whereas for a pressure of 0.43 Pa, the density first decreases, then rises. At high power (550 W), the density gradually increases with increasing magnetic field strength for 0.23 Pa, but for the 0.33 Pa and 0.43 Pa pressures, with increasing magnetic field strength, the density first decreases and then increases, the lowest values all appearing for a magnetic field strength of 52.7 G (1 A).

From sections 3 and 4, with the magnetic field strength changing from 52.7 G (1 A) to 159.1 G (3 A), the mode transition characteristics do not change. At this moment, the density of metastable states near the mode transition point (190 W) changes value from that at higher power ($P_{rf} > 400$ W) to that at lower power ($P_{rf} < 400$ W). For the obvious E-H mode transition occurs, the density of metastable states for the E-mode working condition is no greater than that for the H-mode working condition.

6. Conclusions and summary

By combining HEED data and metastable state densities obtained in optical emission spectroscopy to explore its mechanism, the H mode dependence on the axial static magnetic field (0–318.9 G) were investigated in helical antenna coupling plasma at discharge pressures 0.23–0.43 Pa.

The results show that (a) H-mode characteristics appear and the metastable density increases as magnetic field increase. The reason may be that in the presence of a magnetic field, electrons undergo multiple acceleration-collision cycles that lead to an increase in metastable state density and the efficiency of multiple-step ionization, thereby improving energy utilization. (b) With increasing magnetic field strength, HEED first decrease rapidly and then slowly increase. The competition of the two mechanisms of magnetic field, the radial constraint to the electrons and increasing electric field strength, may lead to this phenomenon. Stronger collisions at higher pressure and greater energy at high RF power lead to the result that the turning point increases at higher pressure and RF power. (c) The HEED decreases with increasing pressure. In a high magnetic field, the energy coupling mechanism changes, which results in a decrease in high-energy electrons at high power as RF power increases. (d) Both the probe data and the metastable variation indicate that electrons tend to be distributed in equilibrium at high RF power. The change in metastable state density with magnetic field indicates that the

magnetic field affects the formation of the H mode by changing the ratio of the density of metastable states under high and low powers.

Data availability statement

The data that support the findings of this study are available upon reasonable request from the authors.

ORCID iD

Xin Lin https://orcid.org/0000-0002-6230-438X

References

[1] Černák M and Ráhel J 2004 *Contrib. Plasma Phys.* **44** 492
[2] Leahy W and Barron V 2006 *J. Adhes.* **77** 215
[3] Arefiev A V and Breizman B N 2004 *Phys. Plasmas* **11** 2942
[4] Boswell R W and Sutherland O 2004 *Phys. Plasmas* **11** 5125
[5] Charles C and Lieberman M A 2006 *Appl. Phys. Lett.* **89** 261503
[6] Díaz F R C 2001 *AIP Conf. Proc.*
[7] Zhang X and Aguirre E 2018 *Phys. Plasmas* **25** 023503
[8] Daltrini A M and Moshkalev S A 2007 *J. Appl. Phys.* **101** 073309
[9] Wegner T and Küllig C 2017 *Plasma Sources Sci. Technol.* **26** 025006
[10] Melazzi D and Lancellotti V 2015 *Plasma Sources Sci. Technol.* **24** 025024
[11] Ellingboe A R and Boswell R W 1996 *Phys. Plasmas* **3** 2797
[12] Lee H-C and Chung C-W 2012 *Thin Solid Films* **521** 185
[13] Ding Z F and Yuan G Y 2008 *Phys. Plasmas* **15** 063506
[14] Wang J and Du Y-C 2014 *Phys. Plasmas* **21** 073502
[15] Razzak M A and Takamura S 2005 *IEEE Trans. Plasma Sci.* **33** 284
[16] Zhang X and Yu P-C 2015 *Phys. Plasmas* **22** 103509
[17] Anderegg F, M H E and Driscoll C F 1998 *Phys. Rev. Lett.* **81** 4875
[18] Lee Y W and Lee H L 2011 *J. Appl. Phys.* **109** 113302
[19] Lee H-C and Lee J-K 2010 *Phys. Plasmas* **17** 033506
[20] Zaplotnik R and Vesel A 2011 *Europhys. Lett.* **95** 55001
[21] Wegner T and Kullig C 2014 *IEEE Trans. Plasma Sci.* **42** 2830
[22] Zhang Z and Zhang X 2018 *IEEE Trans. Plasma Sci.* **46** 3151
[23] Wegner T and Küllig C 2016 *Phys. Plasmas* **23** 023503
[24] Zhang X and Zhang Z-K 2018 *AIP Adv.* **8** 035121
[25] Lieberman M M 1999 *Plasma Sources Sci. Technol.* **8** 313
[26] Lee M-H and Lee K H 2007 *Appl. Phys. Lett.* **90** 191502
[27] Lee M-H and Jang S-H 2006 *Phys. Plasmas* **13** 053502
[28] Lee M-H and Chung C-W 2005 *Phys. Plasmas* **12** 073501
[29] Zheng B, Fu Y and Wen D Q 2020 *J. Appl. Phys.* **53** 435201
[30] Tarey R D and Sahu B B 2012 *Phys. Plasmas* **19** 073520
[31] Sharma N and Chakraborty M 2020 *J. Appl. Phys.* **128** 183303
[32] Chung C, Kim S S and Chang H Y 2004 *Phys. Rev.* E **69** 016406

J. Phys. D: Appl. Phys. **54** (2021) 315201

C Wang *et al*

[33] Godyak V A and Alexandrovich B M 2004 *Phys. Plasmas* **11** 3553

[34] Lee H-J, Yang I-D and Whang K-W 1996 *Plasma Sources Sci. Technol.* **5** 383

[35] Kyeong-Koo Chi T E S and Boswell R W 1999 *Plasma Sources Sci. Technol.* **8** 421

[36] Shamrai K P 1998 *Plasma Sources Sci. Technol.* **7** 499

[37] Shamrai K P and Pavlenko V P 1997 *Plasma Phys. Control. Fusion* **39** 505

[38] Makabe T 2019 *J Phys. D: Appl. Phys.* **52** 213002

[39] Bakowski B and Hancock G 2005 *J. Phys. D: Appl. Phys.* **38** 2769

[40] Malyshev M V and Donnelly V M 1997 *J. Vac. Sci. Technol.* **15** 170

[41] Donnelly V M 2004 *J. Phys. D: Appl. Phys.* **37** R217

[42] Czerwiec T and Graves D B 2004 *J. Phys. D: Appl. Phys.* **37** 2827

[43] Cui R and Han R 2020 *Plasma Sources Sci. Technol.* **29** 015018

[44] Boffard J B and Lin C C 2004 *J. Phys. D: Appl. Phys.* **37** R143

[45] Scheller G R and Gottscho R A 1988 *J. Appl. Phys.* **64** 598

[46] Ferreira C M and Loureiro J 1985 *J. Appl. Phys.* **57** 82

[47] Moshkalyov S A and Steen P G 1999 *Appl. Phys. Lett.* **75** 328

[48] Chen F F and Arnush D 1997 *Phys. Plasmas* **4** 3411

[49] Arnush D and Chen F F 1998 *Phys. Plasmas* **5** 1239

[50] Sun B and Yuan G Y 2010 *Rev. Sci. Instrum.* **81** 054703

[51] Heiler A and Friedl R 2020 *J. Appl. Phys.* **127** 113302